ELSEVIER

Physica D 117 (1998) 145–166

PHYSICA D

Invading wave fronts and their oscillatory wakes are linked by a modulated travelling phase resetting wave

Jonathan A. Sherratt [1]

Department of Mathematics, Heriot-Watt University, Edinburgh EH14 4AS, UK

Received 5 August 1997; received in revised form 8 December 1997; accepted 12 December 1997
Communicated by A.V. Holden

Abstract

Periodic wave trains are the generic solution form for oscillatory reaction–diffusion equations in one space dimension. It has been shown previously that invasive wavefronts generate behind them a wave train with a different speed from that of the invasion [Sherratt, Physica D 70 (1994) 370–382]. In this paper, the mechanism of wave train generation is studied in detail for systems of two reaction–diffusion equations close to a supercritical Hopf bifurcation in the kinetics, with equal diffusion coefficients. A combination of analytical and numerical evidence is presented suggesting that the invasive front and wave train are separated by a modulated travelling wave of phase gradient, in which phase singularities occur periodically. This calculation leads to a prediction of the amplitude and speed of the wave train generated by invasion. Copyright © 1998 Elsevier Science B.V.

Keywords: Oscillatory systems; Wave trains; Reaction–diffusion; Travelling waves

1. Introduction

Periodic wave trains are the generic solution form for oscillatory reaction–diffusion equations in one space dimension. Here 'oscillatory' means that the kinetic ordinary differential equations (ODEs) contain a stable limit cycle, and reaction–diffusion systems with such kinetics are used widely in biological and chemical applications, including the Belousov–Zhabotinskii reaction [1], intracellular calcium signalling [2], and predator–prey interactions [3]. Periodic wave trains (a.k.a. periodic travelling waves) were first studied by Kopell and Howard [4], and over the following two decades, a number of authors studied the existence of such waves, and their stability as solutions of the corresponding reaction–diffusion systems [5–9]. In the last few years attention has shifted to the generation of periodic wave trains from types of initial condition that arise naturally in applications [10,11]. The present paper extends previous work of my own on this question [12], concerning the generation of periodic wave trains behind invasive transition waves. I begin with a brief summary of my previous results.

[1] E-mail: jas@ma.hw.ac.uk.

0167-2789/98/$19.00 Copyright © 1998 Elsevier Science B.V. All rights reserved
PII S0167-2789(97)00317-5

Transition wavefronts of constant shape and speed are one of the most extensively studied solution forms for reaction–diffusion equations, dating back to the ground-breaking work of Kolmogorov et al. [13] and Fisher [14]. Such wavefronts represent the invasion of one equilibrium state by another. The equilibrium ahead of the wave can be either stable or unstable; however, that behind the wave, which I will refer to as the "invading equilibrium", is necessarily stable (see [15] for review). In systems of equations, similar transition fronts are relevant to a wide range of applications [17,18], and numerical evidence for their existence is extensive, although formal proofs are rare, a notable exception being the work of Dunbar [19] on predator–prey models.

In [12], I considered the fate of such transition fronts when kinetic parameters are altered such that the invading equilibrium becomes unstable via a Hopf bifurcation. Although the simple transition front continues to exist formally (at least in some cases), it can clearly no longer be stable. The basic conclusion, based on a series of analytical estimates and numerical simulations, is that the transition front undergoes a bifurcation in parallel with that in the kinetics, into a wavefront behind which there is a periodic wave train. Both the front and the wave train have constant speeds, but these speeds are different, with the wave train moving faster; moreover, the direction of the wave train can be either the same as or opposite to that of the front, depending on parameter values. I will denote the two speeds by c_{front} and c_{train}. A numerical simulation illustrating this behaviour in a predator–prey model is shown in Fig. 1(a). It is important to stress that the work in [12] is not general, and concerns a specific set of equations. However, subsequent studies have shown that this phenomenon, referred to as "oscillatory wakes behind invasion", applies in a wide range of oscillatory reaction–diffusion systems [20,21]. In some cases, one observes highly irregular spatiotemporal oscillations behind a band of periodic travelling waves, as illustrated in Fig. 1(b); this arises when the periodic waves are unstable as solutions of the partial differential equations (PDEs), and the dynamic nature of the irregularities is discussed in detail in [22].

Any oscillatory reaction–diffusion system has a one-parameter family of periodic wave train solutions [4,23], with wave speed or amplitude being convenient parameters. Thus a question raised immediately by the above discussion is: Which member of the wave train family is selected behind the invading front? This question will be answered explicitly in this paper for systems of two reaction–diffusion equations in which the kinetics are close to Hopf bifurcation and in which the diffusion coefficients are equal, via a detailed understanding of the way in which wave trains are generated behind the invading fronts. This understanding builds on partial previous results, which I will now briefly review.

The form of a wavefront with an oscillatory wake is illustrated schematically in Fig. 2. The leading wavefront decays exponentially to the (unstable) invading equilibrium state, and provided that the kinetics are sufficiently close to Hopf bifurcation, the solution remains close to this equilibrium state for a significant distance, before evolving away from the equilibrium, and into a periodic wave train. The phrases "sufficiently close" and "significant distance" are based on previous numerical observations, but will be made analytically precise later in this paper. In [12], I presented numerical evidence that the exponential decay of the leading front, towards the invading equilibrium, plays the central role in wave train selection. This decay has the form of exponentially decaying sinusoidal oscillations, corresponding to a complex eigenvalue with negative real part in the ODEs for travelling wave solutions of speed c_{front}. In [12], I presented numerical evidence indicating that when such an oscillatory decay is applied as a perturbation to the invading equilibrium, it generates a periodic wave train.

In a later paper [24], I investigated this wave train generation in more detail, in the case of reaction–diffusion systems of "λ–ω" type. This class of equations is a standard prototype for oscillatory reaction–diffusion systems; their form facilitates analytical study. I will describe λ–ω systems in detail in Section 2, but a crucial point to mention here is that they cannot be used to study invasion problems as such. This is because invasion requires the existence of two kinetic equilibria, while λ–ω systems have only one. The value of the λ–ω prototype is in studying the effects of perturbations to this one equilibrium, applied as initial conditions. In [24], I considered the particular case of monotone (i.e. non-oscillatory) exponentially decaying perturbations, and showed that such initial data do

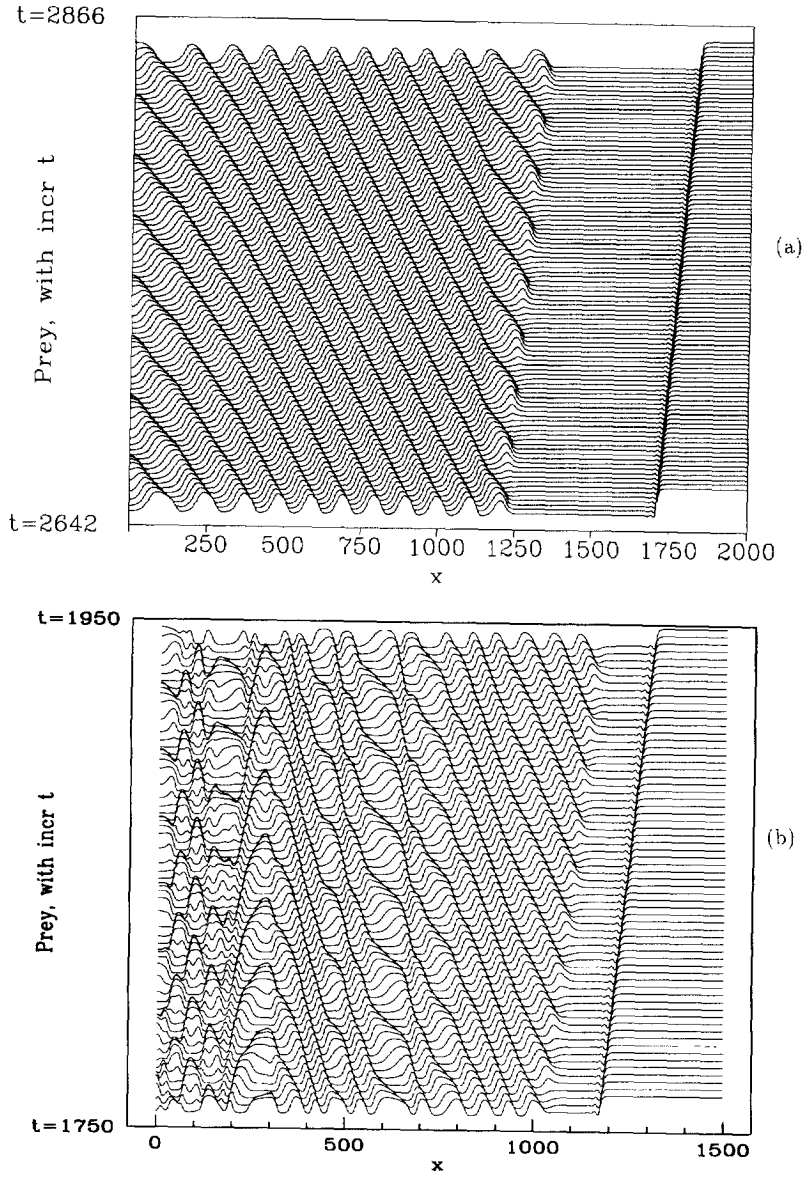

Fig. 1. An illustration of an oscillatory wake behind the simulated invasion of a prey population by predators. The solutions shown are for standard predator–prey models of the form $\partial h/\partial t = \partial^2 h/\partial x^2 + f_h(h, p)$, $\partial p/\partial t = \partial^2 p/\partial x^2 + f_p(h, p)$, with oscillatory kinetics; here h and p denote the prey and predator densities respectively. I plot the prey density h as a function of space at successive times, with the vertical separation of successive solutions proportional to the time interval. The solution for predator density p has a qualitatively similar form. Initially the system is in the prey-only steady state (rescaled to $h = 1$ in both cases) everywhere except near the $x = 0$ boundary, where predators are introduced. This initial perturbation spreads through the domain, corresponding to the invasion of the prey population by predators. Immediately behind the invading wavefront, the solution is close to the (unstable) coexistence steady state, and further back an oscillatory wake develops. In (a) this wake consists of periodic travelling waves; in (b) there are irregular spatiotemporal oscillations, behind a leading band of (unstable) periodic waves. The kinetic functions used are: (a) $f_h(h, p) = h(1-h) - 3hp/(h+0.2)$, $f_p(h, p) = 0.1\,p(1 - p/h)$; (b) $f_h(h, p) = h(1-h) - p(1 - e^{-5h})$, $f_p(h, p) = 0.12\,p(1 - 3e^{-5h})$. These are both standard forms of predator–prey model: their historical origin and applicability is discussed in detail elsewhere [15,16]. In both cases the boundary condition at $x = 0$ is zero flux, $p_x = h_x = 0$, but the qualitative form of the results is independent both of this and of the details of the initial condition. The equations were solved numerically using the method of lines and Gear's method.

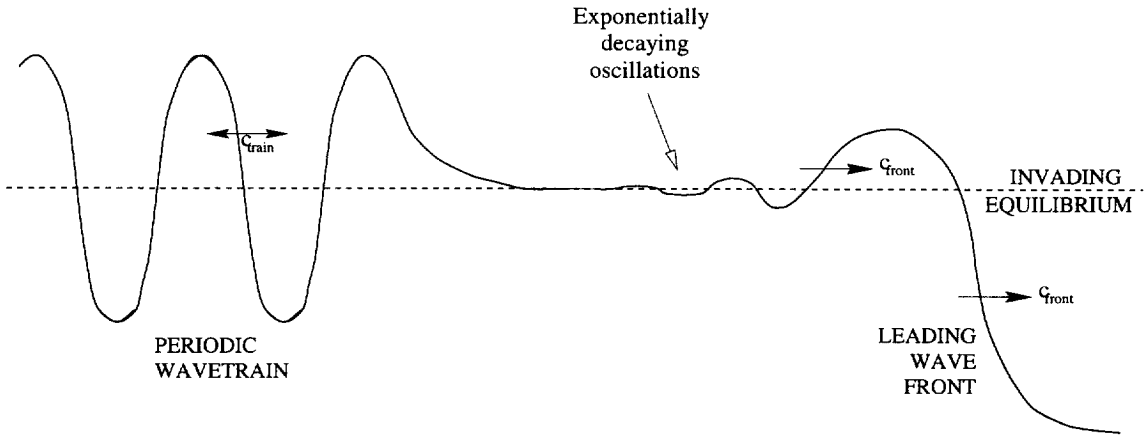

Fig. 2. A schematic illustration of the form of an invading wavefront with an oscillatory wake.

indeed generate a periodic wave train. Moreover, I derived a formula for the amplitude (and thus the speed) of this wave train, as a function of the decay rate of the initial perturbation.

There are three basic and very significant differences between the scenario considered in [24] and the real case of oscillatory wake generation, as discussed in [12]:

(i) The kinetics in general oscillatory reaction–diffusion systems are not of λ–ω form.
(ii) The exponential decay of the leading front to the invading equilibrium is oscillatory rather than monotone.
(iii) This decaying perturbation is applied continuously and moves with the speed of invasion, rather than being applied instantaneously as a stationary initial condition.

The aim of this paper is to bridge these three gaps. I deal with (i) by restricting attention to the case of two coupled reaction–diffusion equations with equal diffusion coefficients, and with kinetic parameter values close to Hopf bifurcation of the invading equilibrium. Then in the neighbourhood of this equilibrium, the kinetics are approximately of Hopf normal form, which gives a λ–ω type system. In Section 2, I address (ii) by generalising the results in [24] to oscillatory perturbations. In Section 3, I extend the work to moving perturbations, in the sense of (iii), by generalising the results further to the case of a moving frame of reference. This will show that the key to wave train selection lies in changes of phase when the solution is close to the invading equilibrium state. In Section 4, I will derive the form of this phase change, which has the form of a modulated travelling wave, in which phase singularities occur periodically in space and time. This is a novel and intrinsically spatiotemporal form of phase resetting. Moreover, the calculation leads to an analytical prediction of the wave train amplitude selected behind invasion.

2. Wave train generation by oscillatory decaying initial data

2.1. Introduction to λ–ω systems

The "λ–ω" class of reaction–diffusion systems has the general form

$$\frac{\partial u}{\partial t} = \frac{\partial^2 u}{\partial x^2} + \lambda(r)u - \omega(r)v, \tag{2.1a}$$

$$\frac{\partial v}{\partial t} = \frac{\partial^2 v}{\partial x^2} + \omega(r)u + \lambda(r)v. \tag{2.1b}$$

Here t denotes time and x denotes space in a one-dimensional domain. In this paper, I will restrict attention to the case

$$\lambda(r) = \lambda_0 - \lambda_1 r^2, \qquad \omega(r) = \omega_0 + \omega_1 r^2, \tag{2.1c}$$

where $\lambda_0, \lambda_1 > 0$, with ω_0, ω_1 taking either sign (but not zero). Two of the parameters λ_0, λ_1, ω_0, and ω_1 can in fact be eliminated by simple rescalings, but since this does not simplify the subsequent analysis, I leave the system in this general form. This is the normal form for kinetics close to a supercritical Hopf bifurcation; all the results in this paper will be based on these forms, and thus apply only sufficiently close to Hopf bifurcation; later I will make the term "sufficiently close" more precise. The case of subcritical Hopf bifurcation is quite different, and has been the subject of fascinating recent work by Ermentrout et al. [11]. Note that (2.1c) implies that the kinetic ODEs have a unique equilibrium point $u = v = 0$, which is unstable, with a stable limit cycle around that point that is circular, with radius $(\lambda_0/\lambda_1)^{1/2}$.

In common with any oscillatory reaction–diffusion system, (2.1) has a one-parameter family of periodic wave train solutions [4]; the beauty of the λ–ω form is that these solutions may be written down explicitly:

$$u = \hat{r}\cos[\omega(\hat{r})t \pm \lambda(\hat{r})^{1/2}x], \qquad v = \hat{r}\sin[\omega(\hat{r})t \pm \lambda(\hat{r})^{1/2}x]. \tag{2.2}$$

Here the wave amplitude $\hat{r}$ parametrises the wave train family; the $\pm$ reflects the fact that the wave train can travel in either the positive or negative x-direction. Moreover, Kopell and Howard [4] derived an exact condition for the stability of (2.2) as a solution of (2.1), namely that

$$4\lambda(\hat{r})\left[1 + \left(\frac{\omega'(\hat{r})}{\lambda'(\hat{r})}\right)^2\right] + \hat{r}\lambda'(\hat{r}) \leq 0 \tag{2.3}$$

for linear stability. Note in particular that waves of sufficiently large amplitude are stable, while those of sufficiently small amplitude are unstable.

Analysis of (2.1) is facilitated by using polar coordinates in the u–v plane, i.e. $r = (u^2 + v^2)^{1/2}$ and $\theta = \tan^{-1}(v/u)$, in terms of which (2.1) becomes

$$r_t = r\lambda(r) + r_{xx} - r\theta_x^2, \tag{2.4a}$$

$$\theta_t = \omega(r) + \theta_{xx} + 2r_x\theta_x/r, \tag{2.4b}$$

$$\lambda(r) = \lambda_0 - \lambda_1 r^2, \tag{2.4c}$$

$$\omega(r) = \omega_0 + \omega_1 r^2, \tag{2.4d}$$

and the periodic travelling wave solution (2.2) is

$$r = \hat{r} \quad \theta = \omega(\hat{r})t \pm \lambda(\hat{r})^{1/2}x. \tag{2.5}$$

The aim of this section is to study the solutions of (2.1) that evolve from exponentially decaying, oscillatory perturbations to the equilibrium state $u = v = 0$. In terms of the invasion problem discussed in Section 1, $u = v = 0$ is analogous to the invading equilibrium, and the initial conditions are analogous to the rear of the invading wavefront. Specifically I consider (2.1) on the semi-infinite domain $-\infty < x < 0$, with initial conditions

$$u(x, 0) = \epsilon\exp(\xi x)\cos(\nu x + \theta_0), \qquad v(x, 0) = \epsilon\exp(\xi x)\sin(\nu x + \theta_0). \tag{2.6}$$

Here $\xi > 0$, and without loss of generality $\nu > 0$; θ_0 and ϵ are constants, with ϵ small relative to the maximum wave train amplitude $(\lambda_0/\lambda_1)^{1/2}$. At the $x = 0$ boundary I use the conditions

$$u_x + \xi u + \nu v = 0 \quad \text{and} \quad v_x + \xi v - \nu u = 0, \tag{2.7}$$

which are satisfied by (2.6), although numerical simulations suggest that Neumann or Dirichlet conditions give essentially identical results except very close to this boundary. I do not attempt a direct analytical determination of the long-term solution of this problem; rather, I present an analytical study of particular solution forms, based on the results of numerical simulations. The work in this section is analogous to that in [24], which considered the case $\nu = 0$; the differences that result from non-zero ν (i.e. oscillatory decay) are important for later sections of the paper.

2.2. *Simulation of evolution from exponentially decaying, oscillatory data*

Numerical solution of λ–ω type reaction–diffusion systems is most easily performed by integrating the u–v equations (2.1) rather than the r–θ equations (2.4). This is because θ is unbounded, which causes great difficulties numerically, although it is of no mathematical significance, since only the value of θ modulo 2π is meaningful. A typical numerical simulation of (2.1) subject to (2.6) and (2.7) is illustrated in Fig. 3. The initial perturbation to the

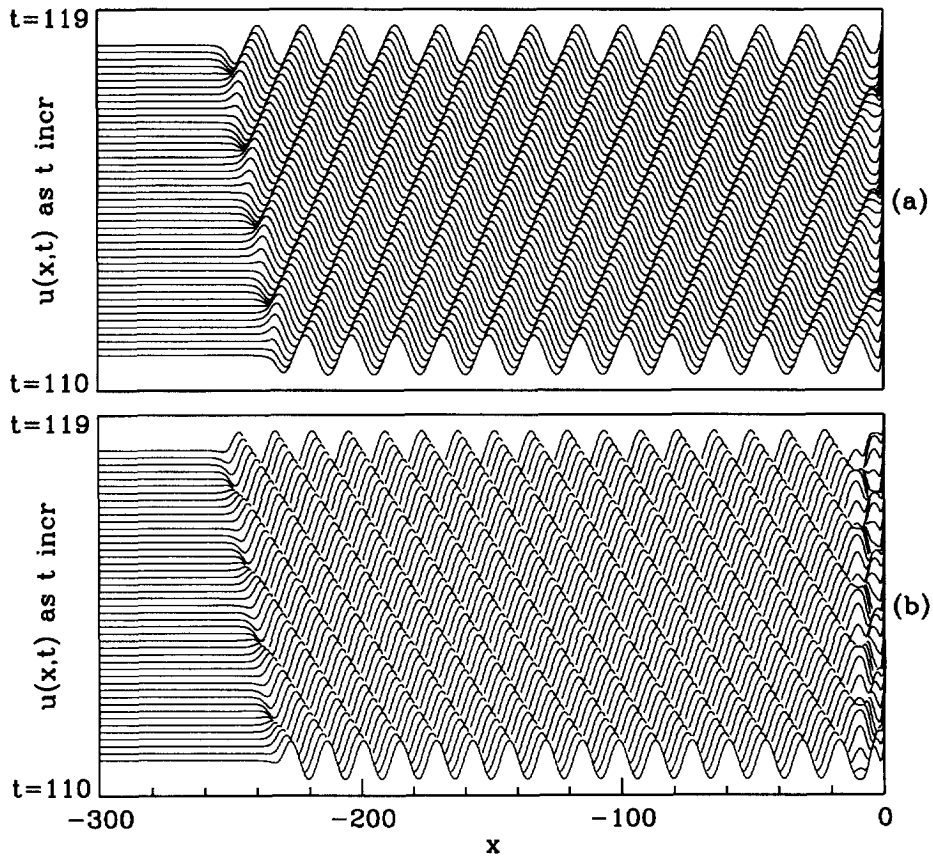

Fig. 3. Periodic wave trains generated by exponentially decaying, oscillatory perturbations to $u = v = 0$ in a λ–ω system. I show the numerical solution of (2.1) subject to (2.6) and (2.7), plotting u as a function of space at successive times, with the vertical separation of successive solutions proportional to the time interval. The parameter values are $\lambda_0 = \lambda_1 = 1$, $\omega_0 = 3$, $\xi = 0.7$, $\nu = 0.15$, $\epsilon = 0.1$ and $\theta_0 = \frac{1}{4}\pi$, with (a) $\omega_1 = -0.1$; (b) $\omega_1 = +0.1$. The initial perturbation spreads across the domain as an amplitude transition front, behind which is a periodic wave train. The front and wave train move at different speeds, in (a) the opposite, and (b) the same, direction. I have used two different numerical methods to solve (2.1), a semi-implicit Crank–Nicolson scheme, and the method of lines and Gear's method. The two methods actually have rather different convergence properties, and their combined use provides a valuable check for the validity of the numerical solutions; details of the methods are given in [25].

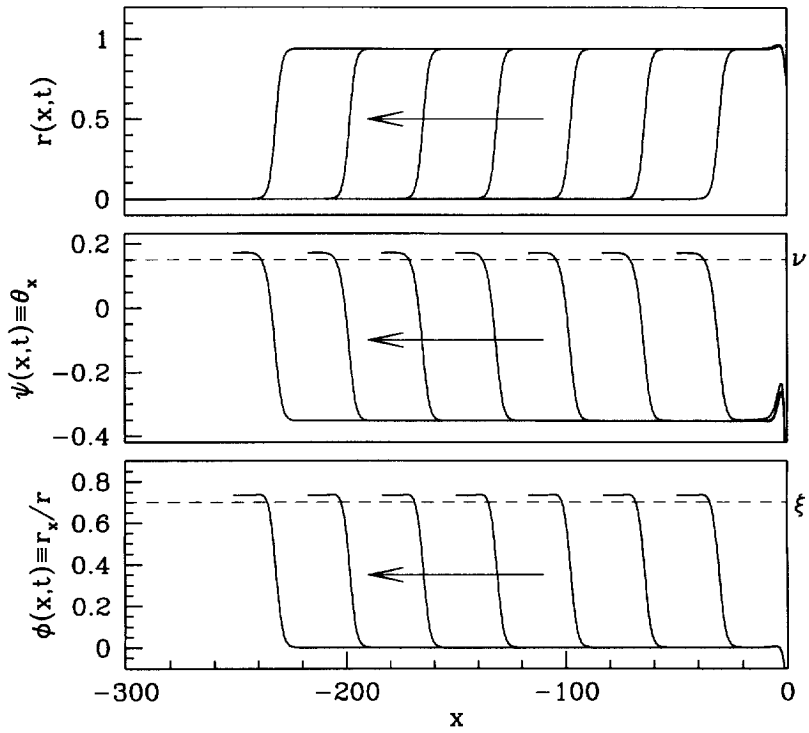

Fig. 4. The solution generated by exponentially decaying, oscillatory perturbations to $u = v = 0$ in a λ–ω system, plotted as r, $\psi \equiv \theta_x$ and $\phi = r_x/r$, rather than as u and v. The solution illustrated is the same as in Fig. 3(a). I plot r, ψ and ϕ, calculated from numerical solutions for u and v, as functions of space at equally spaced times (time interval 15.7). This method of illustration shows that the solution consists of transition wavefronts in r, ψ and ϕ, moving in the negative x-direction with constant shape and speed. The arrows indicate the way in which the solution changes as time increases. The values of ψ and ϕ are not plotted when the numerically calculated solution for r is less than a critical value, taken as 10^{-6}; this avoids values that are unreliable due to rounding errors, which occur both in the PDE solution for u and v and in numerical differentiation of u, v and r.

equilibrium state evolves to a wavefront moving across the domain at constant speed, behind which is a periodic wave train. The wave train has a different speed from the front, and can move in either the positive (as in Fig. 3(a)) or negative (as in Fig. 3(b)) x-directions. It is important to stress that this solution is quite different from that of the invasion problem described in Section 1 and illustrated in Fig. 1, even though both involve a front and wave train moving at different speeds. The essential difference is that the invasion problem arises from the perturbation of an equilibrium point *outside* the limit cycle of the kinetics, while in the present case it is the equilibrium point *inside* the limit cycle that is perturbed.

The basic form of the solution, as illustrated in Fig. 3, is the same in numerical simulations for a wide range of parameters, and appears essentially independent of ϵ and θ_0 except at very early times. Further insight into the solution is given by replotting the solutions as r and $\psi \equiv \theta_x$. This reveals transition wavefronts of constant shape and speed (Fig. 4); behind the front r and ψ are constant, corresponding to periodic travelling waves, and ahead of the front, $r = 0$ and $\psi = \nu$, the value imposed by the initial conditions. It is also convenient to calculate $\phi \equiv r_x/r$, which of course also has the form of a transition wavefront. As illustrated in Fig. 4, $\phi = 0$ behind this front (since r is constant and non-zero), while ahead of the front, $\phi = \xi$, the value imposed by the initial conditions.

2.3. Existence of transition wavefronts

To study this behaviour analytically, I work with the equations in their polar coordinate formulation (2.4), and look for solutions in travelling waveform, $r = \tilde{r}(z_{\text{pert}})$, $\psi(\equiv \theta_x) = \tilde{\psi}(z_{\text{pert}})$, where $z_{\text{pert}} = x + c_{\text{pert}}t$. Here $c_{\text{pert}} > 0$ denotes the speed at which the wavefront, induced by the initial perturbation, moves across the domain. I neglect the $x = 0$ boundary and work on the domain $-\infty < z_{\text{pert}} < \infty$; this is appropriate because the travelling front solutions are relevant to (2.4) as the limiting solutions at large times, and in this limit the $x = 0$ boundary corresponds to $z_{\text{pert}} = +\infty$. The travelling waveform assumed for ψ implies that $\theta = \tilde{\Psi}(z_{\text{pert}}) + F(t)$, where $\tilde{\Psi}(\cdot)$ is an indefinite integral of $\tilde{\psi}(\cdot)$ and $F(\cdot)$ is an arbitrary function of time, that arises as a constant of integration; recall that $\psi \equiv \theta_x$. Substituting this and the travelling waveform for r into (2.4) gives a third-order system of ODEs, which are most conveniently written in terms of the variables $\tilde{r}(z_{\text{pert}})$, $\tilde{\psi}(z_{\text{pert}})$, and $\tilde{\phi}(z_{\text{pert}}) = \tilde{r}'(z_{\text{pert}})/\tilde{r}(z_{\text{pert}})$:

$$\mathrm{d}\tilde{r}/\mathrm{d}z_{\text{pert}} = \tilde{r}\tilde{\phi}, \tag{2.8a}$$

$$\mathrm{d}\tilde{\psi}/\mathrm{d}z_{\text{pert}} = -\omega_0 - \omega_1\tilde{r}^2 + c_{\text{pert}}\tilde{\psi} - 2\tilde{\phi}\tilde{\psi} + f(t), \tag{2.8b}$$

$$\mathrm{d}\tilde{\phi}/\mathrm{d}z_{\text{pert}} = \tilde{\psi}^2 + c_{\text{pert}}\tilde{\phi} - \tilde{\phi}^2 - \lambda_0 + \lambda_1\tilde{r}^2. \tag{2.8c}$$

Here $f(t) = F'(t)$. Eqs. (2.8) were studied originally in [26] for transitions between two wave trains with different (non-zero) amplitudes; here I am considering transitions between solutions with zero and non-zero amplitudes, which have significance differences. The required behaviour at $z_{\text{pert}} = -\infty$ ($\tilde{r} = 0$, $\tilde{\psi} = \nu$, $\tilde{\phi} = \xi$) implies, using (2.8b), that

$$f(t) = \omega_0 - (c_{\text{pert}} - 2\xi)\nu\,, \tag{2.8d}$$

independent of time. The same conditions substituted into (2.8c) imply that

$$c_{\text{pert}} = \xi + (\lambda_0 - \nu^2)/\xi. \tag{2.8e}$$

The transition wavefronts seen in Fig. 3 correspond to heteroclinic connections between steady states of (2.8). I do not attempt a global analysis of such connections, but rather consider simply local stability close to the steady states, which gives a great deal of insight.

Straightforward calculation shows that (2.8) has three steady states with $\tilde{r} \geq 0$:

SS1: $\tilde{r} = 0$, $\tilde{\psi} = \nu$, $\tilde{\phi} = \xi$. This has eigenvalues ξ and $(c_{\text{pert}} - 2\xi) \pm 2\nu\,\mathrm{i}$. Eq. (2.8e) for c_{pert} implies that this steady state is completely unstable if $\xi^2 + \nu^2 < \lambda_0$; otherwise it is a saddle point.

SS2: $\tilde{r} = 0$, $\tilde{\psi} = -\nu$, $\tilde{\phi} = c_{\text{pert}} - \xi$. This has eigenvalues $(c_{\text{pert}} - 2\xi)$ and $(2\xi - c_{\text{pert}}) \pm 2\nu\,\mathrm{i}$, and is thus completely unstable if $\xi^2 + \nu^2 > \lambda_0$, and a saddle point otherwise.

SS3: $\tilde{\psi} = [(c_{\text{pert}} - 2\xi)\nu + \omega_1\tilde{r}^2]/c_{\text{pert}}$, $\tilde{\phi} = 0$, with $\tilde{r}$ satisfying

$$c_{\text{pert}}^2(\lambda_0 - \lambda_1\tilde{r}^2) = [\omega_1\tilde{r}^2 + (c_{\text{pert}} - 2\xi)\nu]^2. \tag{2.9}$$

The number of solutions of (2.9) depends on parameter values. However, I will show shortly that only the case $\nu < \lambda_0^{1/2}$ is of interest, and it is straightforward to show that in this case, there is exactly one real solution for $\tilde{r}$, say $\tilde{r}_s$. The eigenvalues μ at this steady state satisfy

$$\mu^3 - 2c\mu^2 + [c^2 + 4\lambda_0 - 6\lambda_1\tilde{r}_s^2]\mu - \frac{\tilde{r}}{c_{\text{pert}}}\frac{\mathrm{d}}{\mathrm{d}\tilde{r}}[c_{\text{pert}}^2(\lambda_0 - \lambda_1\tilde{r}^2) - (\omega_1\tilde{r}^2 + (c_{\text{pert}} - 2\xi)\nu)^2]\,|_{\tilde{r}=\tilde{r}_s} = 0.$$

Thus the sum of the eigenvalues is positive, while their product is negative, implying that there is one real negative eigenvalue and two others with positive real part.

The transition wavefronts of the type illustrated in Fig. 4 correspond to a heteroclinic connection in (2.8), joining SS3 (at $z_{\text{pert}} = +\infty$) and SS1 (at $z_{\text{pert}} = -\infty$). Since SS3 has only one stable eigenvector, there are two trajectories terminating at the steady state, one of which ($\mathcal{T}_1$, say) has $\tilde{r}$ decreasing to $\tilde{r}_s$, with the other ($\mathcal{T}_2$, say) having $\tilde{r}$ increasing to $\tilde{r}_s$. Numerical integration of (2.8) backwards in z_{pert} as an initial value problem for a wide range of parameter sets, starting close to SS3 on the stable eigenvector, suggests $\tilde{r}$, $\tilde{\psi}$ and $\tilde{\phi}$ all tend to infinity along $\mathcal{T}_1$, while $\mathcal{T}_2$ connects to whichever of SS1 and SS2 is completely unstable. I will assume this behaviour of $\mathcal{T}_2$ in what follows, although it must be remembered that it is only a conjecture, based on (strong) numerical evidence.

It follows that a transition wavefront of the form illustrated in Fig. 3 exists provided SS1 is completely unstable, which requires

$$\xi^2 + \nu^2 < \lambda_0. \tag{2.10}$$

This in turn implies the condition $\nu < \lambda_0^{1/2}$, ensuring exactly one solution of (2.9) with positive non-zero $\tilde{r}$. Thus when condition (2.10) is satisfied, the above analysis suggests that the solution evolves to a transition front in r, ψ and ϕ, moving with speed given by (2.8e), and this is confirmed in numerical simulations (e.g. Fig. 4).

Numerical simulations of the initial value problem (2.1), (2.6), (2.7) show that when condition (2.10) is not satisfied, the solution nevertheless evolves to a transition wavefront in r, ψ and ϕ. The above analysis implies that this front cannot have $\psi = \nu$ and $\phi = \xi$ ahead of it (since no such front exists), and in all cases I have found that this wavefront is that with $\psi = 0$ and $\phi = \lambda_0^{1/2}$ ahead of it, which has speed $2\sqrt{\lambda_0}$. This wavefront is the slowest of those fronts ahead of which $\psi = 0$, and this numerical observation is consistent with the work in [24] which treats only the case $\nu = 0$; however (2.8e) and (2.10) imply that slower fronts do exist for non-zero ν.

2.4. *Stability of transition wavefronts*

The existence of transition wavefronts in r, ϕ and ψ does not, of course, imply that they are stable as solutions of the original reaction–diffusion equations (2.1). Intuitively, one can divide the origin of such instabilities into two categories: either the steady state SS3 (a periodic wave train) behind the front could be unstable, or the front itself could be unstable. The condition for the first of these instabilities was derived in [4] and is given in (2.3), and numerical solutions indicate that as parameters are altered so that SS3 becomes unstable, the transition wavefront solution develops irregular oscillations behind it, corresponding to irregular spatiotemporal oscillations in u and v behind a band of periodic waves.

I end this section by briefly summarising the results of a numerical investigation into the second type of instability. Numerical study is that I calculate the trajectory $\mathcal{T}_2$ by numerical integration of the ODE system (2.8), as explained above. I then use this solution, with some noise added as a small perturbation, as an initial condition in the solution of the PDEs (2.1), and determine whether the solution returns to the travelling front corresponding to $\mathcal{T}_2$, or moves away to a new solution. I have used this procedure previously with success for other amplitude transition fronts in λ–ω systems [27], and in the present case I have performed it for a wide range of parameter sets. Note that ξ and ν are parameters, as well as λ_0, λ_1 and ω_1; the value of ω_0 is irrelevant, since it does not appear in (2.8), and altering its value in (2.1) corresponds to taking two independent linear combinations of (2.1a) and (2.1b).

These simulations indicate that condition (2.10) for the existence of a travelling front solution is not sufficient to ensure its stability. In unstable cases, I have found that, as when (2.10) is not satisfied, the solution evolves to the

front with $\psi = 0$ and $\phi = \lambda_0^{1/2}$ ahead of it. Recall that this front has speed $2\lambda_0^{1/2}$. In the course of running numerical simulations for a wide range of parameter sets, I noticed that the unstable fronts always correspond to a theoretical speed (predicted by (2.8e)) that is less than $2\lambda_0^{1/2}$, suggesting that this may be the condition for stability. In terms of ξ and ν, this condition is

$$\xi + (\lambda_0 - \nu^2)/\xi > 2\sqrt{\lambda_0} \quad \text{i.e. } \xi + \nu < \sqrt{\lambda_0}.$$

(The alternative possibility $\xi > \sqrt{\lambda_0} + \nu$ automatically contravenes condition (2.10)). However, it is important to stress that my evidence for this condition is purely numerical observation; in fact the condition is not required in what follows, and I mention it only for completeness. The essential result of this section is condition (2.10) for the existence of amplitude transition fronts.

3. Wave train generation in a moving frame of reference

In this section, I extend the results of Section 2 to the case of a decaying, oscillatory perturbation that is moving, rather than stationary. This reflects the fact that the decaying tail of the invasive wavefront moves at the speed c_{front}, and is applied continuously, rather than as an instantaneous initial condition (see Fig. 2). To achieve this, I work in a frame of reference moving with speed c_{front} in the positive x-direction, in terms of which the λ–ω system (2.1) has the form

$$\frac{\partial u}{\partial t} = \frac{\partial^2 u}{\partial z_{\text{front}}^2} + c_{\text{front}} \frac{\partial u}{\partial z_{\text{front}}} + \lambda(r)u - \omega(r)v, \tag{3.1a}$$

$$\frac{\partial v}{\partial t} = \frac{\partial^2 v}{\partial z_{\text{front}}^2} + c_{\text{front}} \frac{\partial v}{\partial z_{\text{front}}} + \omega(r)u + \lambda(r)v, \tag{3.1b}$$

$$\lambda(r) = \lambda_0 - \lambda_1 r^2, \tag{3.1c}$$

$$\omega(r) = \omega_0 + \omega_1 r^2. \tag{3.1d}$$

Here $z_{\text{front}} = x - c_{\text{front}} t$. I consider this system on $-\infty < z_{\text{front}} < 0$, with initial conditions

$$u(z_{\text{front}}, t = 0) = \epsilon \exp(\xi z_{\text{front}}) \cos(\nu z_{\text{front}} + \theta_0), \tag{3.2a}$$

$$v(z_{\text{front}}, t = 0) = \epsilon \exp(\xi z_{\text{front}}) \sin(\nu z_{\text{front}} + \theta_0), \tag{3.2b}$$

and boundary condition

$$\frac{\partial u}{\partial z_{\text{front}}} - \xi u + \nu v = 0 \quad \text{and} \quad \frac{\partial v}{\partial z_{\text{front}}} - \xi v - \nu u = 0 \tag{3.3}$$

at $z_{\text{front}} = 0$. These end conditions are precisely (2.6) and (2.7), with x replaced by z_{front}.

It is important to stress that the front speed c_{front} can reasonably be regarded as a parameter in this problem. In a full invasion problem, such as that illustrated in Fig. 1, the invasion speed depends on the kinetics, diffusion coefficients and initial conditions. Full expressions for these dependencies are only available for a few systems of reaction–diffusion equations [28–30]. Crucially, however, these analytical results, together with a large amount of numerical evidence, suggest that the speed depends only on the form of the kinetics close to the equilibrium state being invaded, i.e. the state ahead of the invading front. This is a region of the kinetic phase plane quite separate from the limit cycle, and can thus be regarded as independent. However, it should be remembered that in any particular application, c_{front} will be coupled to λ_0, λ_1, ω_0 and ω_1, with all being functions of the same kinetic parameters.

By contrast, the initial decay rate ξ and wave number ν are not independent parameters, and are functions of λ_0, ω_0 and c_{front}. Derivation of this dependence is straightforward. The initial conditions implied by ξ and ν correspond to the decay of the tail of the invading wavefront towards the invading equilibrium (i.e. $u = v = 0$). This front, and thus its tail, move with the constant speed c_{front}. The ODEs satisfied by such travelling wave solutions with speed c_{front} are given by setting the right-hand sides of (3.1) to zero, and ξ and ν are simply the real and imaginary parts of a complex pair of eigenvalues of these ODEs at $u = v = 0$. Direct calculation of these eigenvalues is possible because the quartic eigenvalue equation factorises easily, giving

$$\xi = \frac{1}{2}\left[-c_{\text{front}} + \left(\frac{1}{2}\left\{c_{\text{front}}^2 - 4\lambda_0 + \sqrt{(c_{\text{front}}^2 - 4\lambda_0)^2 + 16\omega_0^2}\right\}\right)^{1/2}\right], \tag{3.4a}$$

$$\nu = \frac{1}{2}\left[\left(\frac{1}{2}\left\{-c_{\text{front}}^2 + 4\lambda_0 + \sqrt{(c_{\text{front}}^2 - 4\lambda_0)^2 + 16\omega_0^2}\right\}\right)^{1/2}\right]. \tag{3.4b}$$

These are uniquely determined since we are looking for a positive value of ξ; the other pair of eigenvalues (also complex) always has negative real part. In fact, straightforward manipulation shows that the value of ξ implied by (3.4a) is only positive if

$$c_{\text{front}} < \omega_0/\lambda_0^{1/2}. \tag{3.5}$$

As c_{front} passes through this value, the ODEs for travelling waves of that speed pass through Hopf bifurcation at $u = v = 0$; the resulting limit cycle for higher speeds corresponds to a periodic wave train. Thus for $c_{\text{front}} > \omega_0/\lambda_0^{1/2}$, there is the possibility of a periodic wave behind, and moving in parallel with, invasion. Solutions of this type were studied in detail by Dunbar [31], and for invasion speeds above this critical value, the theory of oscillatory wakes that I am describing does not apply, since the solution never approaches the invading equilibrium. However, I have shown previously [20] that in a wide range of ecological applications, c_{front} is significantly below $\omega_0/\lambda_0^{1/2}$ (often by an order of magnitude). Moreover, (3.5) always holds when one is sufficiently close to a Hopf bifurcation point in the kinetics ($\Rightarrow \lambda_0 \ll \omega_0$). In the remainder of this paper, I assume that (3.5) is satisfied.

I have solved (3.1) subject to (3.2) and (3.3) numerically, with ξ and ν given by (3.4), for a wide range of parameter sets. Of course, (3.4) implies that the initial conditions (3.2) are an exact solution of the PDEs when linearised about $u = v = 0$; however, this solution is unstable even in the linear regime (since $u = v = 0$ is unstable), and numerical simulations confirm that any small perturbations grow rapidly. As expected from the results of Section 2, the solution generates a transition wavefront in amplitude r and phase gradient θ_x, moving in the negative x-direction; an example is illustrated in Fig. 5, with $\phi \equiv r_x/r$ also plotted. As is clear in the figure, the moving frame of reference causes a 'gap' to develop between the resulting periodic wave train and the $z_{\text{front}} = 0$ boundary, and another transition wave develops in this gap.

Numerical measurement of the speeds of these two wavefronts in r and θ_x shows that for a wide range of parameters, both move with absolute speed $2\lambda_0^{1/2}$, but in opposite directions. Here the word "absolute" means that these are the speeds with respect to a stationary frame of reference (i.e. in an x-frame rather than a z_{front}-frame). Therefore, unless

$$c_{\text{front}} > 2\lambda_0^{1/2}, \tag{3.6}$$

the transition front moving in the positive x-direction will eventually 'catch up' with the $z_{\text{front}} = 0$ boundary, leading to a more complex solution form. In this case, the theory that I will describe does not apply, and I will assume in the remainder of the paper that (3.6) is satisfied. Note that, as with condition (3.5), (3.6) is always satisfied sufficiently close to Hopf bifurcation in the kinetics. Between the two transition fronts are two bands of periodic waves, of equal

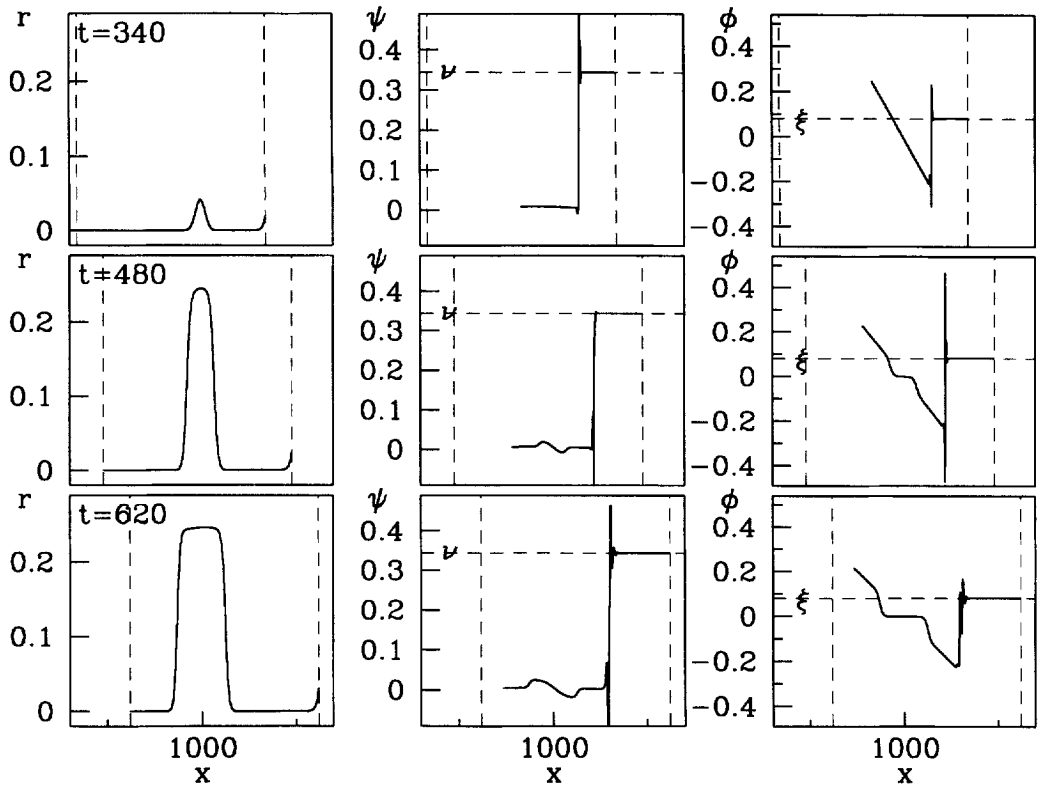

Fig. 5. The solution generated by a moving decaying oscillatory perturbation to $u = v = 0$ in a λ–ω system. I show the solution of (3.1) subject to (3.2) and (3.3), plotting r, $\psi \equiv \theta_x$ and $\phi \equiv r_x/r$ as functions of space at three equally spaced times. The solution consists of two amplitude transition fronts moving in opposite directions but at the same speed, namely $2\lambda_0^{1/2}$ (see main text). Note that for clarity the solutions are plotted in terms of the absolute space variable x, although the equations are actually solved in terms of z_{front} and t; the vertical dashed lines denote the boundaries of the z_{front}-domain on which the equations are solved. As in Fig. 4, the values of ψ and ϕ are not plotted when the numerically calculated solution for r is very small. The parameter values are $\lambda_0 = 0.03$, $\lambda_1 = 0.5$, $\omega_0 = 0.4$, $\omega_1 = 0.15$, and $c_{\text{front}} = 1$.

amplitude but moving in opposite directions, so that the constant values of θ_x are of opposite sign. The interface between these bands is stationary with respect to a stationary frame.

To explain these results, it is simplest to consider the two amplitude transition fronts separately; I consider the front moving in the positive x-direction in Section 4, but first consider that moving in the negative x-direction. This front is directly analogous to those considered in Section 2, being generated by initial data that decay exponentially to $u = v = 0$ as $x \to -\infty$, and the theory presented in Section 2 remains valid even in the moving frame. Thus, in view of condition (2.10) for the existence of amplitude transition fronts, we must consider the value of $\xi^2 + v^2$ relative to λ_0, when ξ and v are given by (3.4). In fact,

$$\begin{aligned} v^2 &= \frac{1}{8}\left[-c_{\text{front}}^2 + 4\lambda_0 + \sqrt{(c_{\text{front}}^2 - 4\lambda_0)^2 + 16\omega_0^2}\right] \\ &> \frac{1}{8}\left[-c_{\text{front}}^2 + 4\lambda_0 + \sqrt{(c_{\text{front}}^2 - 4\lambda_0)^2 + 16\lambda_0 c_{\text{front}}^2}\right] \quad \text{(using (3.5))} \\ &= \lambda_0 \end{aligned}$$

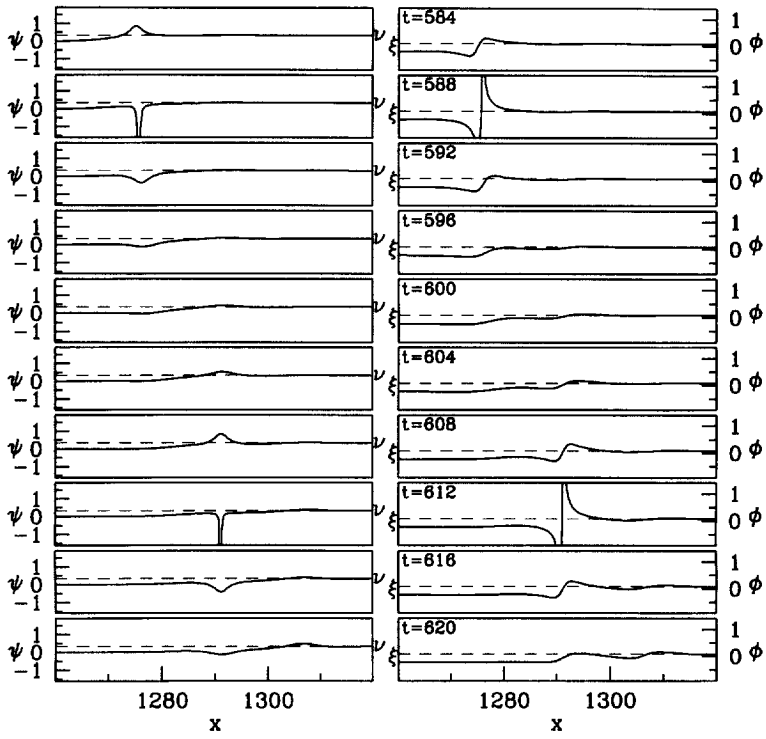

Fig. 6. A more detailed view of the transition in $\psi \equiv \theta_x$ and $\phi = r_x/r$ for the solution shown in Fig. 5. I plot ψ and ϕ for a small range of x-values at 10 successive equally spaced times; note that the time interval is very much shorter than in Fig. 5. The solution has the form of a transition moving in the positive x-direction at a constant speed, but with a shape that varies in time. As in Fig. 5, solutions are plotted in terms of the absolute space variable x, although the equations are actually solved in terms of z_{front} and t. The figure suggests that the temporal variation is actually periodic in a suitable moving frame, and this is confirmed by the analysis in Section 5 of the main text. Note also that there are periodic singularities, occurring once in each time period of the solution, at which ψ and ϕ are infinite; again this is confirmed by the analysis in Section 5 of the main text.

so that (2.10) is never satisfied. Thus the results of Section 2 predict a front speed of $2\lambda_0^{1/2}$, as observed in simulations. Note that in applications, this amplitude transition front moving in the negative x-direction is not usually relevant, since an invasive front is usually generated by applying a perturbation to an unstable equilibrium state, either at a boundary (as in Fig. 1) or localised near one point in the middle of a domain, which is essentially equivalent to perturbing near a boundary on which a symmetry condition is applied. In both cases, the front will reach this boundary almost immediately.

4. Modulated travelling phase resetting waves

The amplitude transition front moving in the positive x-direction requires more careful consideration. In Fig. 5, it is clear that there is a rather complication transition in ψ and ϕ ahead of this transition front; recall that $\psi \equiv \theta_x$ and $\phi \equiv r_x/r$. The key to the explanation of the second transition front lies in understanding this transition. Fig. 6 shows the transition in more detail at a sequence of times. Both ψ and ϕ have the form of a transition front which moves in the positive x-direction, but whose form varies in time.

4.1. An approximate analytical solution

These rather complicated behaviours in ψ and ϕ occur when the amplitude r is very small (see Fig. 5); therefore one anticipates that the nonlinearities in $\lambda(r)$ and $\omega(r)$ are not significant in this behaviour. Exploiting this, I consider the linearised PDE

$$\frac{\partial u}{\partial t} = \frac{\partial^2 u}{\partial {z_a}^2} + a\frac{\partial u}{\partial z_a} + \lambda_0 u - \omega_0 v, \tag{4.1a}$$

$$\frac{\partial v}{\partial t} = \frac{\partial^2 v}{\partial {z_a}^2} + a\frac{\partial v}{\partial z_a} + \omega_0 u + \lambda_0 v. \tag{4.1b}$$

Here $z_a = x - at$, so that I am working in the frame of reference moving in the positive x-direction with an unspecified speed a, denoting the speed of the amplitude transition front moving in the positive x-direction. Determination of this speed is a key goal of this section of the paper, and the method I will use for this depends crucially on working in a frame of reference that moves with the unknown speed. I take $z_a = 0$ to be a point at which this transition front is close to the $u = v = 0$ steady state.

The linearity of this equation raises the possibility of analytical solution, and I will solve the equations using the method of Laplace transforms. The boundary at $z_{\text{front}} = 0$ in Section 3 becomes $z_a = (c_{\text{front}} - a)t$ in the new frame of reference, and such a moving boundary is incompatible with the Laplace transform method. Therefore, I omit this moving boundary, and work instead on the domain $0 < z_a < \infty$, with boundary condition

$$u = h(t)\exp(\xi z_a)\cos(\nu z_a), \quad v = h(t)\exp(\xi z_a)\sin(\nu z_a), \qquad \text{as } z_a \to \infty. \tag{4.2}$$

Here ξ and ν are given by (3.4), and $h(\cdot)$ is an arbitrary function of time; this condition reflects the continuous imposition of oscillatory decay. I will show that the solution of this amended problem does in fact satisfy condition (3.3) to leading order at large times; uniqueness of solutions thus implies that the solution of the original problem (with moving boundary) and that of the amended problem (with boundary at infinity) are the same to leading order at large times. Since I will only be concerned with the leading order behaviour at large times, this change in the problem is valid as a convenient alteration, that facilitates solution.

I consider an initial condition that also reflects oscillatory decay:

$$u = \exp(\xi z_a)\cos(\nu z_a), \quad v = \exp(\xi z_a)\sin(\nu z_a) \qquad \text{at } t = 0. \tag{4.3}$$

To reflect the behaviour as the amplitude transition front approaches $u = v = 0$, I use the boundary condition

$$u_{z_a} + \xi_0 u + \nu_0 v = 0 \text{ and } v_{z_a} + \xi_0 v - \nu_0 u = 0 \qquad \text{at } z_a = 0. \tag{4.4}$$

Recall that $z_a = 0$ is a point at which the transition front is close to $u = v = 0$, and thus ξ_0 and ν_0 represent the real and imaginary components of the eigenvalue along which this decay occurs; $\xi_0 > 0$ necessarily. Based on the results of Section 2, we expect ξ_0, ν_0 and a to be related by

$$a = \xi_0 + (\lambda_0 - \nu_0^2)/\xi_0 \quad \text{with } \xi_0^2 + \nu_0^2 \leq \lambda_0. \tag{4.5}$$

I will solve (4.1) subject to (4.2)–(4.4) using the method of Laplace transforms, and this is made easier by defining

$$w = \exp\left[\frac{az_a}{2} + \left(\frac{a^2}{4} - \lambda_0\right)t - \mathrm{i}\omega_0 t\right](u + \mathrm{i}v), \tag{4.6}$$

where $\mathrm{i} = \sqrt{-1}$. I also write $\alpha = -\xi_0 + \frac{1}{2}a + \mathrm{i}\nu_0$ and $\beta = \xi + \frac{1}{2}a + \mathrm{i}\nu$. In terms of this notation, the problem becomes

$$w_t = w_{z_a z_a} \quad \text{subject to} \quad w_{z_a} = \alpha w \ \text{ at } z_a = 0, \tag{4.7a}$$

$$w = \eta(t)\exp(\beta z_a) \ \text{ as } z_a \to \infty, \tag{4.7b}$$

$$w = \exp(\beta z_a) \ \text{ at } t = 0, \tag{4.7c}$$

where $\eta(\cdot)$ is an arbitrary function of time. Taking the Laplace transform with respect to time t gives a simple ODE, with the following unique solution satisfying the boundary and initial conditions:

$$W(z_a, s) = \frac{1}{2\beta(\beta+\alpha)}\left[\frac{\beta+\alpha}{\sqrt{s}+\beta} + \frac{\beta-\alpha}{\sqrt{s}-\beta} - \frac{2\beta}{\sqrt{s}+\alpha}\right]\mathrm{e}^{-z_a\sqrt{s}} + \frac{\mathrm{e}^{\beta z_a}}{s-\beta^2}.$$

Here I use capital letter to denote Laplace transform, and s is the transform variable. This can be inverted using standard transforms [32], to give

$$w(z_a, t) = \frac{\exp[-{z_a}^2/(4t)]}{2(\beta+\alpha)}\left[2\alpha\mathcal{F}\left(\alpha\sqrt{t} + \frac{z_a}{2\sqrt{t}}\right) + (\beta+\alpha)\mathcal{F}\left(-\beta\sqrt{t} - \frac{z_a}{2\sqrt{t}}\right) + (\beta-\alpha)\mathcal{F}\left(-\beta\sqrt{t} + \frac{z_a}{2\sqrt{t}}\right)\right], \tag{4.8}$$

where $\mathcal{F}(y) \equiv \exp(y^2)\operatorname{erfc}(y)$.

4.2. The value of a

My first application of (4.8) is to determine the speed a of the amplitude transition front moving in the positive x-direction. The key to this lies in the behaviour of the solution at the $z_a = 0$ boundary. Substituting $z_a = 0$ into (4.8) gives

$$w(z_a = 0, t) = \frac{\alpha}{\alpha+\beta}\mathcal{F}(\alpha\sqrt{t}) + \frac{\beta}{(\alpha+\beta)}\mathcal{F}(-\beta\sqrt{t}) \sim \begin{cases} 2\exp(\beta^2 t) - 1/[\beta\sqrt{\pi t}] & \text{if } \alpha = 0, \\ \dfrac{2\beta}{(\alpha+\beta)}\exp(\beta^2 t) & \text{otherwise} \end{cases} \tag{4.9}$$

as $t \to \infty$. Here I am using standard asymptotic expansions for the complimentary error function [32], which imply that

$$\mathcal{F}(z) \sim \frac{1}{z\sqrt{\pi}} + 2\exp(z^2)\mathcal{I}[\operatorname{Re}(z) \le 0] \quad \text{as } t \to \infty, \tag{4.10}$$

where $\mathcal{I}$ denotes the indicator function, defined by $\mathcal{I}[\text{TRUE}] = 1$, $\mathcal{I}[\text{FALSE}] = 0$. Note that (4.5) implies that $\operatorname{Re}(\alpha) \ge 0$. Substituting this asymptotic form for w into (4.6) gives

$$u + \mathrm{i}v|_{z_a=0} \sim \begin{cases} 2\exp(\beta^2 + \mathrm{i}\omega_0)t - \exp(-\mathrm{i}\omega_0 t)/[\beta\sqrt{\pi t}] & \text{if } \alpha = 0, \\ \dfrac{2\beta}{(\alpha+\beta)}\exp[(\beta^2 + \lambda_0 - a^2/4 + \mathrm{i}\omega_0)t] & \text{otherwise} \end{cases} \quad \text{as } t \to \infty.$$

Therefore, if $\alpha \neq 0$,

$$r|_{z_a=0} \sim \frac{2\beta}{(\alpha+\beta)} \exp[(a - c_{\text{front}})\xi t] \tag{4.11a}$$

as $t \to \infty$, while if $\alpha = 0$,

$$r|_{z_a=0} \sim |2\exp[(2\lambda_0^{1/2} - c_{\text{front}})(\xi + \mathrm{i}\nu)t + \mathrm{i}\omega_0 t] - 1/[\beta\sqrt{\pi t}]| \sim 1/[\beta\sqrt{\pi t}] \tag{4.11b}$$

as $t \to \infty$, using (3.6). Here I have substituted $\beta = \xi + \frac{1}{2}a + \mathrm{i}\nu$, and replaced ξ and ν by the expressions in (3.4); recall that $r = (u^2 + v^2)^{1/2} \equiv |u + \mathrm{i}v|$.

In the framework I am considering, the $z_a = 0$ boundary represents a fixed point on the right-moving amplitude transition wave. Therefore, it is necessary that r approaches a constant on that boundary at large times; this is in addition to the constancy of ψ and ϕ, which is implied by the boundary condition (4.4). Eq. (4.11) implies that $r(z_a = 0, t \to \infty)$ is constant at large times in two possible cases:

Case (i): $a = c_{\text{front}}$. This implies that $\alpha \neq 0$, using (3.6). This would mean that the right-moving amplitude transition wave moves in parallel with the invasive front, a fixed distance behind it. Such a solution of the caricature problem (4.1) subject to (4.2)–(4.4) exists for any ξ_0 and ν_0 satisfying (4.5). However, I have never observed this situation in numerical solutions of (3.1) subject to (3.2) and (3.3). I have no quantitative argument for why this is, but intuitively one expects that amplitude transition waves moving faster than the minimum speed $2\lambda_0^{1/2}$ will only arise when ξ_0 and ν_0 are imposed by the initial data, which is not the case here.

Case (ii): $a = 2\lambda_0^{1/2}$. This is required for $\alpha = 0$, and implies that $\xi_0 = \lambda_0^{1/2}$ and $\nu_0 = 0$. Further, this is the case observed in numerical simulation. Eq. (4.11) actually implies that $r \to 0$ as $t \to \infty$ in this case, but this approach to zero is only algebraic, with r being proportional to $t^{-1/2}$. This decay can be corrected by subtracting a factor proportional to $(\log t)/t$ ($\to 0$ as $t \to \infty$) from the wave speed: such a correction is familiar from Fisher's equation, for which compactly supported initial data have exactly this weak convergence to a travelling front [33]. The easiest way to see this is to consider the large time behaviour of the solution at $z_a = -\frac{1}{2}\log t$ rather than at $z_a = 0$; although I have solved the equations on $0 < z_a < \infty$, the solution is well defined for negative values of z_a. This has no affect on the large time form for w, which is still given by (4.9); i.e. $w(z_a = -\frac{1}{2}\log t,\ t) \sim w(z_a = 0,\ t)$ as $t \to \infty$. However, conversion to $u + \mathrm{i}v$ has the effect of multiplying the large time behaviour at $z_a = 0$ by $t^{1/2}$; thus $r(z_a = -\frac{1}{2}\log t,\ t) \sim t^{1/2} r(z_a = 0,\ t) \sim 1/\left[\beta\sqrt{\pi}\right]$ as $t \to \infty$, a non-zero constant as required.

4.3. *Large time solution for ψ and ϕ*

I now consider the large time behaviour of (4.8) at other values of z_a. Although the previous calculation implies $\alpha = 0$, I leave α general, to highlight that in fact the long time behaviour of ϕ and ψ is independent of α. Specifically, I will determine the behaviour as $t \to \infty$ with $z_a \sim 2\gamma t$; here γ is an arbitrary, strictly positive constant. Applying (4.10) to (4.8) gives

$$w(z_a, t) \sim \exp\{-\gamma^2 t\}\left[\exp\{(\beta+\gamma)^2 t\} + \frac{\beta-\alpha}{\beta+\alpha}\exp\{(-\beta+\gamma)^2 t\}\mathcal{I}[\gamma \leq \mathrm{Re}(\beta)]\right.$$
$$\left. + \frac{2\alpha}{\alpha+\beta}\exp\{(\alpha+\gamma)^2 t\}\cdot\mathcal{I}[\gamma \leq -\mathrm{Re}(\alpha)] + \frac{\kappa}{\sqrt{\pi t}}\right] \tag{4.12}$$

as $t \to \infty$ with $z_a \sim 2\gamma t$. Here $\kappa = \gamma(\beta - \alpha)/[(\alpha + \gamma)(\gamma^2 - \beta^2)]$. Note in particular that since I am assuming $\gamma > 0$, it follows that $\kappa \neq 0$; the case $\gamma = 0$ would correspond to points with z_a fixed, i.e. to a frame of reference moving with the left-hand boundary.

As mentioned above, (4.5) implies that $\mathrm{Re}(\alpha) \geq 0$, so that the final term in (4.12) never makes a contribution. Note that $\mathrm{Re}(\beta) = \xi + \frac{1}{2}a$ and is thus strictly positive. Moreover, $\mathrm{Re}[(\beta+\gamma)^2] > \mathrm{Re}[(-\beta+\gamma)^2]$, since $\mathrm{Re}(\beta)$ and γ are both strictly positive, with γ real. Thus (4.12) implies that to leading order,

$$w(z_a,t) \sim \exp\{-\gamma^2 t\}\left[\frac{\kappa}{\sqrt{\pi t}} + \exp\{(\beta+\gamma)^2 t\}\right] \tag{4.13}$$

as $t \to \infty$ with $z_a \sim 2\gamma t$. In this expression, the first term in the square brackets will dominate if $\mathrm{Re}[(\beta+\gamma)^2] < 0$, and the second term will dominate otherwise. Note that $\mathrm{Re}[(\beta+\gamma)^2] < 0 \Leftrightarrow \gamma < \gamma^* \equiv \mathrm{Im}(\beta) - \mathrm{Re}(\beta)$, since γ, $\mathrm{Im}(\beta)$ and $\mathrm{Re}(\beta)$ are all positive.

I am principally interested in ψ ($\equiv \theta_x$) and ϕ ($\equiv r_x/r$), rather than u and v as such. These are easily related to w, however, since

$$\phi + \mathrm{i}\psi = (w_{z_a}/w) - (a/2) = -(a/2) + \frac{1}{2tw}\left.\frac{\partial w}{\partial \gamma}\right|_{t \text{ constant}}. \tag{4.14}$$

Substituting (4.13) into (4.14) and simplifying implies that, to leading order as $t \to \infty$,

$$\begin{aligned}\phi + \mathrm{i}\psi &\sim -(a/2) - \gamma + \frac{\sqrt{\pi t}\,(\beta+\gamma)\exp\{(\beta+\gamma)^2 t\}}{\kappa + \sqrt{\pi t}\exp\{(\beta+\gamma)^2 t\}} \\ &= -(a/2) - \gamma + \frac{\sqrt{\pi t}\,(\beta+\gamma)\mathcal{A}}{\kappa\exp\{-2\mathrm{i}\,\mathrm{Im}(\beta)[\gamma + \mathrm{Re}(\beta)]t\} + \sqrt{\pi t}\,\mathcal{A}},\end{aligned} \tag{4.15}$$

where $\mathcal{A} = \exp\{(\gamma-\gamma^*)[\gamma + \mathrm{Re}(\beta) + \mathrm{Im}(\beta)]t\}$; recall that $\gamma^* = \mathrm{Im}(\beta) - \mathrm{Re}(\beta)$. Since $\gamma + \mathrm{Re}(\beta) + \mathrm{Im}(\beta)$ is strictly positive, the large-time behaviour depends on the sign of $\gamma - \gamma^*$:

if $\gamma > \gamma^*$:

$$\phi + \mathrm{i}\psi \sim -(a/2) - \gamma + (\beta+\gamma) = \xi + \mathrm{i}\nu, \quad \text{i.e.} \quad \phi \sim \xi, \quad \psi \sim \nu,$$

if $\gamma < \gamma^*$:

$$\phi + \mathrm{i}\psi \sim -(a/2) - \gamma = -(z_a + at)/(2t) \quad \text{i.e.} \quad \phi \sim x/2t, \quad \psi \sim 0.$$

It is exactly the transition between these two limiting states that is illustrated in Fig. 6. Note that the behaviour for $\gamma > \gamma^*$ implies that $w_{z_a} \sim \beta w$ at $z_a = (c_{\mathrm{front}} - a)t$, in accordance with condition (3.3). It is this that justifies by replacement of the moving boundary at $z_a = (c_{\mathrm{front}} - a)t$ with a boundary at $z_a = \infty$ in the present calculation.

To understand the transition in more detail, I consider the behaviour for $\gamma = \gamma^*$ in more detail; specifically, I take $z_a = 2\gamma^* t + \zeta + o(t)$ as $t \to \infty$. Thus ζ, which is $\mathrm{O}_s(1)$ as $t \to \infty$, is a lower order correction to z_a in the specific case $\gamma = \gamma^*$. Here I am using the notation $X = \mathrm{O}_s(Y) \Leftrightarrow X = \mathrm{O}(Y)$ and $Y = \mathrm{O}(X)$. Replacing γ by $\gamma^* + \frac{1}{2}\zeta/t$ in (4.15) gives

$$\begin{aligned}\phi + \mathrm{i}\psi &\sim -(a/2) - \gamma^* - \tfrac{1}{2}\zeta/t \\ &\quad + \frac{\sqrt{\pi t}\,(\beta+\gamma^*+\frac{1}{2}\zeta/t)\exp\{(\frac{1}{2}\zeta/t)[\frac{1}{2}\zeta/t + 2\,\mathrm{Im}(\beta)]t\}}{\kappa\exp\{-2\mathrm{i}\,\mathrm{Im}(\beta)[\frac{1}{2}\zeta/t + \mathrm{Im}(\beta)]t\} + \sqrt{\pi t}\exp\{(\frac{1}{2}\zeta/t)[\frac{1}{2}\zeta/t + 2\,\mathrm{Im}(\beta)]t\}} \\ &\sim -(a/2) - \gamma^* + \frac{\sqrt{\pi t}\,(\beta+\gamma^*)\exp\{\mathrm{Im}(\beta)\zeta\}}{\kappa\exp\{-\mathrm{i}\,\mathrm{Im}(\beta)[\zeta + 2\,\mathrm{Im}(\beta)t]\} + \sqrt{\pi t}\exp\{\mathrm{Im}(\beta)\zeta\}} \\ &= -(a/2) - \gamma^* + \frac{(\nu + \mathrm{i}\nu + a/2)\exp\{(1+\mathrm{i})\nu\zeta + \frac{1}{2}\log t\}}{(\kappa/\sqrt{\pi})\exp\{-2\mathrm{i}\nu^2 t\} + \exp\{(1+\mathrm{i})\nu\zeta + \frac{1}{2}\log t\}}.\end{aligned} \tag{4.15a}$$

Here

$$\zeta = 2t(\gamma - \gamma^*) = z_a - 2[\,\mathrm{Im}(\beta) - \mathrm{Re}(\beta)]t = z_a - [2(\nu - \xi) - a]\,t; \tag{4.15b}$$

recall that $\beta = \xi + \frac{1}{2}a + \mathrm{i}\nu$. The $\log t$ term in the exponentials is clearly a lower order correction at large times, and thus to leading order the solution (4.15) is a function of both ζ and time t, with the explicit t-dependence being periodic, with period π/ν^2. The variable ζ is a travelling wave coordinate, corresponding to the wave speed $[2(\nu - \xi) - a]$ in a z_a-frame, and thus to the speed $2(\nu - \xi)$ in an absolute (x-) frame.

A solution such as (4.15), which is temporally periodic in a particular moving frame, is known as a "modulated travelling wave". Modulated waves were first studied by Rand [34] in the context of rotating waves in fluids; more recent work has also been primarily in fluid dynamics [35,36], although an interesting application to spiral waves in forced excitable media has recently been published [37]. The modulated travelling waveform (4.15) agrees very closely with the solution form determined in numerical simulations of (3.1), such as that illustrated in Fig. 6. In particular, both the wave speed and temporal period compare well for a wide range of parameter sets; this confirms the relevance of the various approximations used to derive (4.15).

It is clearly important to consider how the speed $2(\nu-\xi)$ compares with the various other wave speeds in the problem, notably the invasion speed c_{front}, and $2\lambda_0^{1/2}$, which is the speed of the right-moving amplitude transition front. Using (3.4), it is straightforward to see that $2(\nu-\xi)$ is always strictly positive, and also strictly less than c_{front}. Moreover,

$$\begin{aligned}
2(\nu - \xi) > 2\lambda_0^{1/2} \iff & \left[(c_{\mathrm{front}}^2 - 4\lambda_0) + \sqrt{(c_{\mathrm{front}}^2 - 4\lambda_0)^2 + 16\omega_0^2}\right]^{1/2} \\
& - \left[-(c_{\mathrm{front}}^2 - 4\lambda_0) + \sqrt{(c_{\mathrm{front}}^2 - 4\lambda_0)^2 + 16\omega_0^2}\right]^{1/2} < \sqrt{2}\left(c_{\mathrm{front}} - 2\sqrt{\lambda_0}\right) \\
\iff & \left[(c_{\mathrm{front}}^2 - 4\lambda_0) + \sqrt{(c_{\mathrm{front}}^2 - 4\lambda_0)^2 + 16\omega_0^2}\right] \\
& + \left[-(c_{\mathrm{front}}^2 - 4\lambda_0) + \sqrt{(c_{\mathrm{front}}^2 - 4\lambda_0)^2 + 16\omega_0^2}\right] - 8\omega_0 < 2\left(c_{\mathrm{front}} - 2\sqrt{\lambda_0}\right)^2 \\
& \quad \text{and} \quad c_{\mathrm{front}} > 2\sqrt{\lambda_0} \\
\iff & \sqrt{(c_{\mathrm{front}}^2 - 4\lambda_0)^2 + 16\omega_0^2} < 4\omega_0 + \left(c_{\mathrm{front}} - 2\sqrt{\lambda_0}\right)^2 \quad \text{and} \quad c_{\mathrm{front}} > 2\sqrt{\lambda_0} \\
\iff & (c_{\mathrm{front}}^2 - 4\lambda_0)^2 < 8\omega_0\left(c_{\mathrm{front}} - 2\sqrt{\lambda_0}\right)^2 + \left(c_{\mathrm{front}} - 2\sqrt{\lambda_0}\right)^4 \\
& \quad \text{and} \quad c_{\mathrm{front}} > 2\sqrt{\lambda_0} \\
\iff & c_{\mathrm{front}} < \omega_0/\sqrt{\lambda_0} \quad \text{and} \quad c_{\mathrm{front}} > 2\sqrt{\lambda_0}.
\end{aligned}$$

These two conditions are just (3.5) and (3.6), which I am already assuming to hold. Thus the modulated travelling wave moves in the positive x-direction, at a speed that is greater than that of the right-moving amplitude transition front but less than the invasion speed c_{front}.

An interesting property of the solution (4.15) is that it has a singularity once in each time period. Specifically, ϕ and ψ are both infinite whenever

$$\kappa \exp\{-2\mathrm{i}\nu^2 t\} + \exp\{(1 + \mathrm{i})\nu\zeta\} = 0$$

(here I am neglecting the $\log t$ term, which is appropriate at large times). This complex equation can be rewritten as two real equations, which determine ζ uniquely, and determine t up to an arbitrary multiple of π/ν^2, the temporal period of the wave; thus

$$x = x_0 + n \cdot 2(\nu - \xi)\pi/\nu^2, \quad t = t_0 + n \cdot \pi/\nu^2 \qquad (n \in \mathbb{Z})$$

for some x_0 and t_0 depending on initial data. At these points, u and v are both instantaneously zero, so that the solution passes through the origin of the u–v plane. These points are thus "phase singularities", since the phase θ is undefined, and in fact θ has a jump of π as one follows the solution through such a point, as a function of either space or time; this is exactly as expected for a solution passing through the origin.

At large times, I have found that my numerical calculations of the transition in ψ and ϕ break down, giving irregularities indicative of numerical noise, rather than the modulated wave observed at small times (such as in Fig. 6). The solution (4.13) actually explains this phenomenon, since it implies that a typical value of the solution amplitude r, at the location of the modulated transition wave, decreases exponentially in time, according to $r \propto \exp[-\{(\nu - \xi)^2 - \lambda_0\}t]$. Thus although ψ and ϕ are temporally periodic in an appropriately moving frame, r is not. Clearly r will in due course decrease sufficiently that its value, and consequently the calculated values of ψ and ϕ become dominated by truncation errors. Specifically, one expects this to occur at time $t \approx \ln \mathcal{E}/[(\nu - \xi)^2 - \lambda_0]$, where $\mathcal{E}$ is the truncation error. Using an estimate of the truncation error for my numerical methods, I have found that this predicted time agrees well with the time at which noise begins to dominate the calculated transition in ψ and ϕ.

5. Discussion

In this paper, I have studied the phenomenon of oscillatory wakes, in which periodic wave trains develop behind invasive wavefronts. In fact I have not considered the full invasion problem at all, but rather, I have used a series of caricature problems to predict the details of the solution behind the invasive front. Because of the form of caricature problems used, the work applies only when the reacting variables have the same diffusion coefficients, and only close to a supercritical Hopf bifurcation in the kinetics; however, there are no restrictions on the functional forms of the kinetics. Within these constraints, my results make the following predictions:

(1) The oscillatory wake phenomenon depends centrally on the solution being close to the invading equilibrium for a significant distance behind the invading front. This imposes the condition $c_{\text{front}} > 2\lambda_0^{1/2}$, and when the front speed is below this value, different mechanisms apply.

(2) It is also necessary that the invasion speed is sufficiently slow that there are no periodic wave trains solutions of that speed; this requires $c_{\text{front}} < \omega_0/\lambda_0^{1/2}$.

(3) When these two conditions are satisfied, and when the kinetics are sufficiently close to Hopf bifurcation that the λ–ω form is a good approximation, the behaviour behind invasion will have the form determined in this paper. The invading front decays exponentially towards the invading equilibrium; this decay moves with constant shape and constant speed c_{front}. However, it is interrupted by a modulated travelling phase resetting wave, which includes periodic phase singularities, and which moves with speed $2(\xi - \nu)$, where ξ and ν are defined in (3.4). Behind this phase resetting wave, the phase evolves gradually to a point at which $\theta_x = -\lambda_0^{1/2}$, which is at the foot of an amplitude transition front. This transition front itself moves with speed $2\lambda_0^{1/2}$.

(4) Behind this transition front is a periodic wave train, which is that observed behind invasion. Its amplitude R is given as the unique solution of

$$4\lambda_0(\lambda_0 - \lambda_1 R^2) = \omega_1^2 R^4,$$

which is the appropriate version of (2.9), with unique positive solution

$$R = \left[\frac{2\lambda_0}{\omega_1^2}\left(\sqrt{\lambda_1^2 + \omega_1^2} - \lambda_1\right)\right]^{1/2}. \qquad (5.1)$$

This prediction of wave train amplitude behind invasion is one of the central results of this paper. Of particular interest is that (5.1) is independent of the invasion speed c_{front}, and is a function only of the form of the reaction kinetics near the invading equilibrium. The fact that (5.1) is independent of ω_0 is expected, since this parameter affects only the phase of the solutions, not their amplitude.

It is important to emphasise that I have not in any sense proved that (5.1) gives the amplitude of periodic wave trains behind invasion; rather, I have studied a number of caricature models, both analytically and numerically, which suggest that (5.1) applies close to Hopf bifurcation. With this proviso, expression (5.1) is a valuable tool in a number of applications, enabling a number of key aspects of the behaviour behind invasions to be related to model parameters. In particular:

- *Speed and direction of the wave train behind invasion.* The speed of the periodic wave train whose amplitude is given by (5.1) is

$$c_R = |\omega(R)|/\sqrt{\lambda(R)} = 2\sqrt{\lambda_0} + \frac{|\omega_0\omega_1|}{\sqrt{\lambda_0}}\left(\sqrt{\lambda_1^2+\omega_1^2}-\lambda_1\right)^{-1}.$$

This expression passes through zero as parameters are changed so that the direction of the wave train changes: determining the appropriate sign of θ_x shows that the wave train moves in the same direction as the invasion if and only if

$$\frac{\omega_0}{2\lambda_0} < \frac{\lambda_1 - \sqrt{\lambda_1^2+\omega_1^2}}{\omega_1}.$$

Note that while the parameter ω_0 does not affect the amplitude of the wave train, it does affect the velocity of the corresponding waves.

- *Stability of the wave train behind invasion.* Substituting (5.1) into condition (2.3) for wave train stability in λ–ω systems implies that periodic waves behind invasion will be stable if and only if

$$\begin{aligned}
&\sqrt{\lambda_1^2+\omega_1^2}-\lambda_1 < \frac{\lambda_1^3}{\lambda_1^2+\omega_1^2}\\
&\iff \left(\frac{\omega_1}{\lambda_1}\right)^6 + 2\left(\frac{\omega_1}{\lambda_1}\right)^4 - \left(\frac{\omega_1}{\lambda_1}\right)^2 - 3 < 0\\
&\iff \frac{|\omega_1|}{\lambda_1} < 1.0714\ldots,
\end{aligned}$$

since the cubic polynomial has a unique positive real root. Note that this result is independent of λ_0, and therefore both stable and unstable wave trains are possible arbitrarily close to Hopf bifurcation in kinetics.

The latter condition for stability is particularly important in application to ecological invasions, because it enables the space of ecological parameters to be divided into cases of stable and unstable wave trains behind invasion. I have shown previously that when an unstable wave train is selected, the result is spatiotemporal irregularity behind invasion [12], and in the context of ecology, preliminary evidence indicates that the selection of either regular or irregular oscillations is the major determinant of the long-term behaviour after an entire domain has been invaded [20]. The results also have important applications to intracellular calcium signalling, where the "invasion" of regions of low calcium density by higher densities is a key mechanism in the coordination of the behaviour of an individual cell or a group of cells [2,38]. In this case, the relationship between the invasion speed and the behaviour behind invasion is an important benchmark for testing, against experimental data, the various mathematical models in current use [39].

The work described in this paper applies only close to a standard supercritical Hopf bifurcation in the kinetics. It is important to emphasise that more complicated kinetic bifurcations do often arise in applications, and an example of this is provided by the recent work of Merkin and Sadiq [40]. They consider the behaviour behind invasive wavefronts in a cubic autocatalysis system, modelled as two coupled reaction–diffusion equations. These equations do have a standard supercritical Hopf bifurcation in one region of parameter space, but elsewhere the kinetics are more complex, including supercritical Hopf bifurcations, periodic orbit bifurcations and the co-existence of nested stable and unstable limit cycles. These very rich kinetics give a wide range of different spatiotemporal behaviours behind invasion, which are explored in detail (numerically) in [40]; the present paper is relevant to only one parameter region for this model. Another recent study focussing on a different type of oscillatory reaction–diffusion system is that of Ermentrout et al. [11]. They consider wave train generation and interaction close to a subcritical Hopf bifurcation point, demonstrating a wide range of behaviours, including transition fronts between wave trains and homogeneous oscillations, and spatially localised oscillations. All of these complex behaviours are due to complex bifurcation structures in the kinetics. The results in this paper provide a detailed understanding of the generation of periodic wave trains behind invasion in the simpler case of a system close to supercritical Hopf bifurcation, a case with a range of important applications in biology and chemistry.

Acknowledgements

I am grateful to Dwight Barkley, John Dallon and Pam Wiener for helpful discussions.

References

[1] R. Kapral, K. Showalter, Chemical Waves and Patterns, Kluwer Academic Publishers, Dordrecht, 1995.
[2] J. Sneyd, J. Keizer, M.J. Sanderson, Mechanisms of calcium oscillations and waves: A quantitative analysis, FASEB J. 14 (1995) 1463–1472.
[3] E.E. Holmes, M.A. Lewis, J. Banks, R.R. Veit, Partial differential equations in ecology: Spatial interactions and populations dynamics, Ecology 75 (1994) 17–29.
[4] N. Kopell, L.N. Howard, Plane wave solutions to reaction–diffusion equations, Stud. Appl. Math. 52 (1973) 291–328.
[5] H.G. Othmer, Current problems in pattern formation, Lect. Math. Life Sci. 9 (1977) 57–86.
[6] G.B. Ermentrout, Small amplitude stable wave trains in reaction–diffusion systems, Lect. Notes Pure Appl. Math. 54 (1980) 217–228.
[7] K. Maginu, Stability of periodic travelling wave solutions with large spatial periods in reaction–diffusion systems, J. Diff. Eqns. 39 (1981) 73–99.
[8] T.M. Kapitula, Stability of weak shocks in λ–ω systems, Indiana Univ. Math. J. 40 (1991) 1193–1219.
[9] S. Koga, Coexistence of stably propagating periodic wave trains in intrinsically bistable reaction–diffusion systems, Phys. Lett. A 191 (1994) 251–256.
[10] S. Koga, A variety of stable persistent waves in intrinsically bistable reaction–diffusion systems – from one-dimensional periodic-waves to one-armed and 2-armed rotating spiral waves, Physica D 84 (1995) 148–161.
[11] B. Ermentrout, X. Chen, Z. Chen, Transition fronts and localized structures in bistable reaction–diffusion systems, Physica D 108 (1997) 147–167.
[12] J.A. Sherratt, Irregular wakes in reaction–diffusion waves, Physica D 70 (1994) 370–382.
[13] A. Kolmogorov, I. Petrovsky, N. Piscounov, Etude de l'équation de la diffusion avec croissance de la quantité de matière et son application à un problème biologique, Moscow Univ. Bull. Math. 1 (1937) 1–25.
[14] R.A. Fisher, The wave of advance of advantageous genes, Ann. Eugenics 7 (1937) 353–369.
[15] J.D. Murray, Mathematical Biology, Springer, Berlin, 1989.
[16] R.M. May, Stability and Complexity in Model Ecosystems, Princeton University Press, Princeton, NJ, 1981.
[17] A. Okubo, Dynamical aspects of animal grouping: swarms, schools, flocks and herds, Adv. Biophys. 22 (1986) 1–94.
[18] P.D. Dale, P.K. Maini, J.A. Sherratt, Mathematical modelling of corneal epithelial wound healing, Math. Biosci. 124 (1994) 127–147.
[19] S.R. Dunbar, Travelling wave solutions of diffusive Lotka–Volterra equations: A heteroclinic connection in R^4, Trans. AMS 286 (1984) 557–594.

[20] J.A. Sherratt, B.T. Eagan, M.A. Lewis, Oscillations and chaos behind predator–prey invasion: mathematical artifact or ecological reality?, Phil. Trans. Roy. Soc. B 352 (1997) 21–38.
[21] J. Sneyd, J.A. Sherratt, On the propagation of calcium waves in an inhomogeneous medium, SIAM J. Appl. Math. 57 (1997) 73–94.
[22] J.A. Sherratt, Unstable wave trains and chaotic wakes in reaction–diffusion systems of λ–ω type. Physica D 82 (1995) 165–179.
[23] R.J. Field, M. Burger (Eds.), Oscillations and Travelling Waves in Chemical Systems, Wiley, New York, 1985.
[24] J.A. Sherratt, On the evolution of periodic plane waves in reaction–diffusion equations of λ–ω type. SIAM J. Appl. Math. 54 (1994) 1374-1385.
[25] J.A. Sherratt, A comparison of two numerical methods for oscillatory reaction–diffusion equations, Appl. Math. Lett. 10 (1997) 1–5.
[26] L.N. Howard, N. Kopell, Slowly varying waves and shock structures in reaction–diffusion equations, Stud. Appl. Math. 56 (1977) 95–145.
[27] J.A. Sherratt, On the speed of amplitude transition waves in reaction–diffusion equations of λ–ω type, IMA J. Appl. Math. 52 (1994) 79–92.
[28] M.I. Freidlin, On wavefront propagation in multicomponent media, Trans. AMS 276 (1983) 181–191; see also the erratum, Trans. AMS 289 (1985) 429.
[29] M. Freidlin, Coupled reaction–diffusion equations, Ann. Prob. 19 (1991) 29–57.
[30] J. Billingham, D.J. Needham, The development of travelling waves in quadratic and cubic autocatalysis with unequal diffusion rates. III: Large time development in quadratic autocatalysis, Quart. Appl. Math. 50 (1992) 343–372.
[31] S.R. Dunbar, Travelling waves in diffusive predator–prey equations – periodic orbits and point-to-periodic heteroclinic connections, SIAM J. Appl. Math. 46 (1986) 1057–1078.
[32] M. Abramowitz, I.A. Stegun, Handbook of Mathematical Functions, Dover, New York, 1970.
[33] F. Rothe, Convergence to travelling fronts in semilinear parabolic equations, Proc. Roy. Soc. Edin. A 80 (1978) 213–234.
[34] D. Rand, Dynamics and symmetry. Predictions for modulated waves in rotating fluids, Arch. Rat. Mech. Anal. 79 (1982) 1–37.
[35] M. Myers, P. Holmes, J. Elezgaray, G. Berkooz, Wavelet projections of the Kuramoto–Sivashinsky equation. 1. Heteroclinic cycles and modulated waves for short systems, Physica D 86 (1995) 396–427.
[36] S.M. Cox, Mode interactions in Rayleigh–Benard convection, Physica D 95 (1996) 50–61.
[37] R. Mantel, D. Barkley, Periodic forcing of spiral waves in excitable media, Phys. Rev. E 54 (1996) 4791–4802.
[38] D.E. Clapham, J. Sneyd, Intracellular calcium waves, Adv. Second Mess. Phosphoprotein Res. 30 (1995) 1–24.
[39] Y.H. Tang, J.L. Stephenson, H.G. Othmer, Simplification and analysis of models of calcium dynamics based on IP3-sensitive calcium channel kinetics, Biophys. J. 70 (1996) 246–263.
[40] J.H. Merkin, M.A. Sadiq, The propagation of travelling waves in an open cubic autocatalytic chemical system, IMA J. Appl. Math. 57 (1996) 273–309.